JPET Fast Forward. Published on August 10, 2012 as DOI: 10.1124/jpet.112.197756

JPET #197756

Title: Target Binding Properties and Cellular Activity of Afatinib (BIBW 2992), an Irreversible ErbB Family Blocker

Authors: Flavio Solca, Goeran Dahl, Andreas Zoephel, Gerd Bader, Michael Sanderson, Christian Klein, Oliver Kraemer, Frank Himmelsbach, Eric Haaksma, Guenther R. Adolf

Primary laboratory of origin: Boehringer Ingelheim RCV GmbH & Co

Author affiliations:

Boehringer Ingelheim RCV GmbH & Co KG, Vienna, Austria (F.S., G.D., A.Z., G.B., M.S., C.K., O.K., E.H. and G.R.A.)

Boehringer Ingelheim Pharma GmbH & Co. KG., Biberach/Riss, Germany (F.H.)

JPET Fast Forward. Published on August 10, 2012 as DOI: 10.1124/jpet.112.197756
This article has not been copyedited and formatted. The final version may differ from this version.

Running title page

Running title: Afatinib, an irreversible inhibitor of EGFR, HER2 and ErbB4

Corresponding author: Flavio Solca

Address: Doktor-Böhringer-Gasse 5-11, A-1120, Vienna, Austria
Telephone: + 43-1-801-05-2298
Fax: +43-1-801-05-32298
E-mail: flavio.solca@boehringer-ingelheim.com

Number of text pages: 44
Figures and tables: 5 figures and 1 table
Number of references: 37
Number of words in the Abstract: 250/250
Number of words in the Introduction: 665/750
Number of words in the Discussion: 981/1,500

Abbreviations:

AKT, AKT8 virus oncogene cellular homolog: ATP, adenosine triphosphate; EGF, epidermal growth factor; EGFR, epidermal growth factor receptor; $EGFR^{WT}$, epidermal growth factor receptor wild-type (synonymous to EGFR); $EGFR^{L858}$, epidermal growth factor receptor L858R mutant; $EGFR^{L858R/T790M}$, epidermal growth factor receptor L858R/T790M double mutant; ErbB, proto-oncogene B of the avian erythroblastosis virus AEV-H strain (ErbB1 encodes EGFR); GST, glutathione-S-transferase; HER1, human epidermal growth factor receptor 1 also known as EGFR or ErbB-1; HER2, human epidermal growth factor receptor 2 also known as ErbB-2; HER3, human epidermal growth factor receptor 3 also known as ErbB-3; HER4, human epidermal growth factor receptor 4 also known as ErbB-4; JAK, janus kinase; MAPK, mitogen-activated protein kinase; mTOR, mammalian target of rapamycin; PBS, phosphate buffered saline; PI3K, phosphoinositide 3 kinase; PLC, phospholipase C; PKC, protein kinase C; RAF, rapidly accelerated fibrosarcoma; RAS, oncogene originally discovered in rat sarcoma; SPR, surface plasmon resonance; STAT, signal transducer and activator of transcription

Recommended section assignment: Cellular and molecular

JPET Fast Forward. Published on August 10, 2012 as DOI: 10.1124/jpet.112.197756
This article has not been copyedited and formatted. The final version may differ from this version.

ABSTRACT

Deregulation of the ErbB receptor network is well recognized as an oncogenic driver in epithelial cancers. Several targeted drugs have been developed, including antibodies and small molecule kinase inhibitors, each of them characterized by distinct patterns of ErbB receptor interactions. Understanding the precise pharmacological properties of these compounds is important for optimal use in clinical practice. Afatinib (BIBW 2992) is an ATP-competitive anilinoquinazoline derivative harboring a reactive acrylamide group and was designed to covalently bind and irreversibly block enzymatically active ErbB receptor family members. Here we show by X-ray crystallography the covalent binding of afatinib to wild-type EGFR and by mass spectrometry the covalent interaction with EGFR, $EGFR^{L858R/T790M}$, HER2 and ErbB-4. Afatinib potently inhibits the enymatic activity of ErbB-4 (EC_{50} = 1 nM) and the proliferation of cancer cell lines driven by multiple ErbB receptor aberrations at concentrations below 100 nM. BI 37781, a close analog of afatinib lacking the acrylamide group and thus incapable of covalent bond formation, had similar potency on cells driven by EGFR or $EGFR^{L858R}$, but less or no detectable activity on cells expressing $EGFR^{L858R/ T790M}$ HER2 or ErbB-4. These results stress the importance of the acrylamide group and show that afatinib differs from approved ErbB targeting agents by irreversibly inhibiting the kinase activity of all ErbB family members.

They provide a mechanistic rationale for the distinct pharmacological features of this compound and explain the clinical activity seen in some patients resistant to antibody or kinase inhibitor therapy due to secondary mutations or ErbB receptor ‘reprogramming’.

Introduction

The ErbB signaling network plays a central role in epithelial tissue development and homeostasis. At least ten different ligands regulate the activity of ErbB receptors, which signal as ligand-induced dimers formed by four related transmembrane receptor tyrosine kinases, EGFR/ErbB-1/HER1, HER2/ErbB-2/neu, HER3/ErbB-3 and HER4/ErbB-4. In the absence of ligand, the extracellular domains of EGFR, ErbB-3 and ErbB-4 adopt an autoinhibited conformation. Ligand binding triggers a conformational change in the extracellular domain and masked dimerization residues become exposed at the protein surface thus allowing homo- and/or heterodimerization. HER2 differs from other family members by lacking a reported ligand and by the fact that its extracellular domain is permanently poised in an 'active-like' conformation (Garrett et al., 2003; Graus-Porta et al., 1997). Although controversially discussed (Alvarado et al., 2009), it has therefore been proposed that HER2 is the preferred heterodimerization partner for other family members (Graus-Porta et al., 1997).

Receptor dimerization results in the formation of asymmetrical (tail-to-head) complexes of the partnered catalytic domains. In such dimers, one monomer acts as an allosteric activator and induces activation of the intrinsic catalytic activity of the partnered receptor (Zhang et al., 2006). Specific tyrosine residues within the C-terminal regulatory domain of the activating partner become transphosphorylated and subsequently act as docking sites for adaptor proteins,

which engage multiple signaling pathways including the RAS/RAF/MAPK, the PI3K/AKT/mTOR, the JAK/STAT as well as the PLCγ/PKC cascades. The exact nature of the intracellular signal depends on the signaling context, the particular ErbB dimers formed and thus on expression of ErbB receptors and their ligand(s) (Tzahar et al., 1996).

Aberrant signaling through the ErbB growth factor receptor system is found in many types of epithelial cancers (Yarden and Sliwkowski, 2001; Zhang et al., 2007). Receptor mutations and/or gene amplifications as well as overproduction of particular ligands are amongst the best described oncogenic mechanisms. EGFR mutations that disrupt the inactive extracellular conformation (e.g. EGFR variant type III [EGFRvIII]) or induce/stabilize the active form of the intracellular catalytic domain (e.g. L858R point mutation or exon 19 deletions) have been identified and validated as cancer-promoting mechanisms (Ji et al., 2006; Lynch et al., 2004). Similarly, HER2 gene amplification has been observed in breast and gastric cancer, and ErbB4 mutations have been described in tumor samples from non-small cell lung cancer, melanoma, breast and colon cancer patients (Slamon et al., 1987; Bang et al., 2009; Prickett et al., 2009).

The increased understanding of the role of ErbB receptor deregulation in cancer promotion triggered the development of a number of therapeutic agents. The armamentarium of approved ErbB-directed drugs includes specific antibodies that prevent ligand binding and/or receptor dimerization (e.g. cetuximab targeting EGFR, trastuzumab specific for HER2) as well

as molecules targeting the intrinsic catalytic activity of ErbB receptors (e.g. gefitinib, erlotinib or lapatinib). Additional inhibitors are currently in clinical development. These low molecular weight compounds generally bind to the ATP pocket of the enzymes, but show remarkable diversity in their potency for inhibition of different ErbB family members and EGFR mutant isoforms. While some inhibitors bind reversibly to either the inactive or the active conformation of the kinase domains, others contain a reactive chemical group potentially allowing the formation of a covalent bond to the active site of the target (Eck and Yun, 2010).

Understanding the selectivity and binding mode of an ErbB-directed small molecule is an important prerequisite for its optimal use in the clinical setting. In contrast to currently approved ErbB kinase inhibitors with reversible binding mode (i.e. erlotinib, gefitinib and lapatinib), afatinib which is currently being assessed in clinical Phase III trials in lung, breast, and head and neck cancer patients (Li et al., 2008; www.clinicaltrials.gov) contains an electrophilic group capable of Michael addition to conserved cysteine residues within the catalytic domains of EGFR (Cys^{797}), HER2 (Cys^{805}) and ErbB-4 (Cys^{803}). Here we show for the first time that afatinib covalently binds to its targets and irreversibly inhibits their enzymatic activity which results in inhibition of ErbB-4 and long lasting cellular activity.

Materials and Methods

Cell Culture and Reagents. All cells were obtained from the American Type Culture Collection and cultured according to the provider's instructions. Masterstocks have been generated and authenticated by SNP chip analysis using the Sanger Institute databases as reference. ErbB kinase domains 0102-0000-1 (EGFR), 0724-0000-1 ($EGFR^{T790M}$), 0725-0000-1 ($EGFR^{T790M/L858R}$), 0108-0000-1 (ErbB2) and 0109-0000-1 (ErbB4) were obtained as expressed glutathione-S-transferase (GST)-fusion proteins in Sf9 cells (ProQinase, GmbH, Germany).

Surface Plasmon Resonance Evaluation. Surface Plasmon Resonance (SPR) monitoring mass density changes was used to measure drug–target interactions. All SPR experiments were performed by Beactica AB, Uppsala, Sweden, on a Biacore T100 instrument (Biacore AB, Uppsala, Sweden). GST-His6-tagged kinase domains (H672-A1210) of EGFR for wild type ($EGFR^{WT}$) and the L858R/T790M variant (ProQinase, Freiburg, Germany) were injected over a CM3 sensor chip (Biacore AB, Uppsala, Sweden), coated with Anti-His6 antibodies (GE Healthcare), using 25 mM HBS (Sigma), 0.05% Tween-20 (BHD/Prolado) pH 7.4 as running buffer. All interaction experiments were carried out at 25°C at a final DMSO concentration of 5% (v/v) in running buffer at a flow rate of 30 µl/min. The pH of this running

buffer was adjusted to pH 7.0 or 8.0 using sodium hydroxide. Compounds were analyzed at 200 nm concentration using 300 s contact time followed by 600 s dissociation time. All measurements were performed at least three times. Data were analyzed using the Biacore T100 software 2.0 or the BIA evaluation software 4.1 (Biacore AB, Uppsala, Sweden). Reference and blank subtracted data were corrected for baseline drift and normalized prior to data analysis. The interaction models were fitted to the data for each compound and protein surface separately. For $EGFR^{WT}$, up to 1,000 response units of protein with high (70–100%) surface activity could be reached, whereas capturing of the $EGFR^{L858R/T790M}$ variant resulted in lower surface activity (30–50%). None of the compounds tested were found to interact with the immobilized capture antibodies in the concentration range used (data not shown).

Protein Production for Crystallography and Data Analysis. Protein preparation and crystallographic work was done by Proteros Biostructures GmbH, Germany. The protein kinase domain of the human epidermal growth factor receptor (EGFR-KD, Gly696-Gly1022, numbering according to SwissProt entry P00533) was cloned in pFastBac 1 as a thrombin-celavable GST-fusion. Recombinant baculovirus was produced using the Bac-to-Bac-system and the protein was expressed by infection of Sf9 cells with high titer virus stock in 10L single-use bioreactors (Wave Biotech). Cells were controlled for infection and

viability, harvested 48–64 hours after infection and stored at –80°C until purification. For purification, cells were thawed in 40 mL lysis buffer (1 x PBS supplemented with 10% glycerol, 5 mM ß-mercaptoethanol and protease inhibitor tabs) per liter of culture medium and lysed using an Ultra-Turrax device. After centrifugation, the lysate was loaded onto a glutathione sepharose column (GE Health Care) equilibrated in lysis buffer without protease inhibitor and bound protein was eluted using 20 mM Tris/Cl, pH=8.0, 150 mM NaCl, 10% glycerol, 10 mM GSH, 5 mM DTT. The GST-tag was removed using Thrombin (GE Health Care) and EGFR-KD was separated from GST by a second passage over the same column. The flow-through of this column was pooled and EGFR-KD was purified to >90% homogeneity as judged by SDS-PAGE on a Superdex75 column (GE Health Care) equilibrated in 50 mM Tris/Cl, pH=8.0, 500 mM NaCl, 10% glycerol and 5 mM DTT. For crystallization, the protein was buffer-exchanged using NAP25-columns (GE Health Care).

The T790M-mutant was generated using the QuikChange™ Site-Directed Mutagenesis Kit (Stratagene) and the mutant protein was produced following the protocols for the wild type.

Crystallization of wild-witype EGFR-KD performed similar to previously described procedures (Stamos et al., 2002). Prior to crystallization protein was concentrated to a final concentration of 12mg/ml in 20mM TRIS 8.0, 0.1mM benzamidine and 1mM DTT. This buffer was also used for protein dilution before crystallization. The sample was filtrated before set-up

up of drops (0.22 µm centrifugal filter units, Millipore). Crystals of wild-type EGFR-KD with benzamidine were produced by vapor diffusion setup. Drops were set as follows: 0.5 µl protein (8 mg/ml, dilution buffer see above) was mixed with 0.5 µl of reservoir solution in hanging drops. The reservoir solution contained 1.4 M KNaTartrate, 0.1 M HEPES, pH7.0 and 2 mM DTT. Crystals appeared after 1 day incubation at 20°C. For soaking crystals were transferred to a solution containing 5 mM afatinib, 1.5 M KNaTartrat, 0.1 M HEPES, pH 7 and 5% DMSO. Crystals were soaked overnight by transfer to 25% glycerol in reservoir and direct freezing in liquid nitrogen.

For crystallization of the T790M mutant, Prior to crystallization 1µM of afatinib was added to the protein before concentrating the protein to a final concentration of 8 mg/ml in the buffer containing 50 mM TRIS pH8.0, 500 mM NaCl, 10% Glycerin and 5 mM TCEP. Crystals of EGFR-KD were produced by vapor diffusion setup. Drops were set as follows: 0.5 µl protein was mixed with 0.5 µl of reservoir solution in hanging drops. The reservoir solution contains 27 % PEG6000, 0.3 M NaCl, 0.1 M HEPES, pH8.0 and 5 mM TCEP (Yun et al., 2008). Crystals appeared overnight at 20°C. The X-ray diffraction data was collected from co-crystals of EGFR or $EGFR^{T790M}$ with afatinib at the SWISS LIGHT SOURCE synchrotron facility (SLS, Villigen, Switzerland) under cryogenic conditions. Data were processed using the XDS package (Kabsch, 2010). The phase information necessary to determine and analyze the

structures was obtained by molecular replacement. A published model of EGFR (Protein Data Base PDB accession code 1M17, Stamos et al., 2002) was used as a search model. Subsequent model building and refinement was performed according to standard protocols with the CCP4 (Collaborative Computational Project, Number 4, 1994) and COOT (Emsley et al., 2010) software packages. Statistics of the final structures and the refinement processes are listed in the Supplementary Material. The coordinates of EGFR and $EGFR^{T790M}$ complexed with afatinib as well as the respective structure factors have been deposited at the protein database under the PDB accession codes 4G5Jand4G5P.

Mass Spectrometric Analyses. The recombinant enzymes EGFR, $EGFR^{T790M/L858R}$, HER2 and ErbB-4 (ProQinase, Freiburg, Germany) tagged with a GST-His-tag were captured on a Ni-IMAC column (Ni-NTA Superflow Qiagen # 101840) and washed with 50 mM HEPES pH 7.5 (4-(2-hydroxyethyl)-1-piperazineethanesulfonic acid) buffer to remove glutathione and dithiothreitol (DTT). The immobilized proteins were incubated with a 10-fold (EGFR isoforms) to 20-fold molar excess of afatinib for 60 (EGFR isoforms) or 120 minutes at 37°C and free afatinib was removed by washing before pepsin cleavage. Peptic peptides were collected from the supernatant after centrifugation, separated on a C18 column (Phenomenex, Luna C18) and collected for Electrospray Ionization Tandem Mass Spectrometry (ESI-MS)

analysis (Dionex Ultimate 3500 NCS). Chemically synthesized peptides covalently modified with afatinib corresponding to the pepsin cleavage product were used as reference for high performance liquid chromatography (HPLC) and ESI-MS analyses.

Kinase Inhibition Assays. Non-radioactive *in vitro* kinase assays were performed as previously described (Solca et al., 2004; Li et al., 2008). The final ATP concentrations were adjusted individually to saturation (50 µM for EGFR and 250 µM for HER2). ErbB-4 kinase activity was determined in a radioactive kinase assay format (Solca et al., 2004; Li et al., 2008) at a final ATP concentration of 50 µM.

Transient Transfection Experiments. The full length ErbB-4 receptor (transcript variant JM-a/CVT-1 with accession number NM_005235) was cloned into the pCMV6-XL4 vector (GenBank Accession Number: AF067196) and used for transient transfection experiments in NIH-3T3 cells. Expression of ErbB-4 was time dependent and maximal 48 hours post-infection. Cellular assays were performed as described in the respective section. HER4 was detected by western blot analyses from transfected cell extracts using a rabbit mAb HER4/ErbB4 clone 83B10 (Cell Signaling #4792).

Cellular EGFR and HER2 Phosphorylation Assays. The enzyme-linked immunosorbent assay (ELISA) methods used for assessing EGFR and HER2 phosphorylation in cellular models were previously reported (Solca et al., 2004; Li et al., 2008). In brief, 1 x 10^4 near confluent A431 cells (ATCC, CRL-1555), NCI-H1975 (ATCC, CRL-5908) or 2 x 10^4 (BT474, HTB-20) were used for the ELISA experiments**.** For phospho-EGFR determination serial dilutions of compounds were incubated for 1 hour prior EGF-stimulation (Promega, G5021; 100 ng/ml) for 10 minutes at room temperature. Cells were washed two times with ice cold PBS before extraction as previously described. To detect HER2 phosphorylation in BT474 cells ligand stimulation was not necessary as these cells display constitutive HER2 phosphorylation under the culture conditions. Therefore, a 100 µl aliquot of 2X HEPEX buffer was directly added to each well after the 1 hour incubation period with compounds. Extractions were performed on a microtiter plate shaker for 1 hour.

Cellular Proliferation Assays. The effect of ErbB inhibitors on cellular proliferation was tested in various assay formats including anchorage-dependent (BT474 cells grown on plastic, 2D assays) and -independent (NCI-H1975 cells grown in soft-agar, 3D assays) assays. BT474 growing in DMEM (Bio Whittaker, 12-604F) were harvested, counted and used for the fluorescence assay according to the method of Dengler et al. Briefly, 2 x10^4 cells were seeded in

90 µl medium in each well of a 96-well flat-bottomed microtiter in presence of serial dilutions of test compounds diluted in 10 % dimethyl sulfoxide/PBS to a final assay concentration of 1%. The concentration of the test compounds covered a range between 50 µM and 0.8 nM. Each drug concentration was plated in duplicate. After 96 hours of continuous drug exposure non-viable cells were stained by addition of 25 µl/well of a propidium iodide solution (50 µg/ml). The basal fluorescence (FU1) was measured after 10 minutes of incubation in the dark using a Labsystems Fluoroskan II micro-plate reader (excitation 544 nm, emission 612 nm). After measurement, the culture medium was removed and cells were permeabilized by freezing the plates at –80°C for at least 90 minutes. After thawing, propidium iodide (100 µl/well of 12.5 µg/ml) was added to the plates which were incubated for 10 minutes at room temperature in the dark. A second fluorescence measurement (FU2) was taken to estimate the amount of total cells. The number of viable cells was calculated as difference between these two measurements (FU2-FU1). The data were analyzed using the program PRISM (GraphPad Inc.). The inhibitor concentrations were transformed to logarithmic values and the raw data were normalized. The normalized values were used to calculate the EC_{50} by a nonlinear regression curve fit (sigmoidal dose-response (variable slope). NCI-H1975 (ATCC, CRL-5908) cells were grown in RPMI1640 medium supplemented with 10% fetal calf serum and prepared for 3D assays (0.3% sea plaque agarose top layer) as described in Li et al., 2008.

Results

Biochemical and biophysical characterization of kinase inhibitor interactions

The inhibitory profile of afatinib in biochemical EGFR and HER2 kinase assays has previously been reported (Li et al., 2008). Afatinib is a highly potent inhibitor of wild-type EGFR (EC_{50} = 0.5 nM) and HER2 (14 nM) and the oncogenic mutants $EGFR^{L858R}$ (0.4 nM) and $EGFR^{L858R/T790M}$ (10 nM), the latter known to be associated with resistance to approved EGFR inhibitors like erlotinib. We have now expanded these observations to include assessments on ErbB-4 inhibitory activity as well as a comparison with structurally distinct ErbB kinase inhibitors. Furthermore, we have designed, synthesized and profiled BI 37781, a compound with close structural similarity to afatinib that lacks the reactive double bond and thus is incapable of forming a covalent bond to the catalytic site cysteine residues (Figure 1). The new biochemical data (Table 1) reveals that afatinib also potently inhibits the kinase activity of ErbB-4 with an EC_{50} of 1 nM. In comparison to afatinib, BI 37781 which showed similar potency on wild-type EGFR was 5-fold less active on the L858R EGFR mutant, the $EGFR^{L858R/T790M}$, HER2 and, most strikingly, on ErbB-4 with a 500-fold loss (EC_{50} = 544 nM). For comparison (Table 1), we included additional EGFR inhibitors in our assays. Canertinib, a kinase inhibitor containing a reactive acrylamide group, showed a selectivity profile similar to afatinib, whereas the reversible inhibitors gefitinib and erlotinib – similar to BI 37781 –

JPET Fast Forward. Published on August 10, 2012 as DOI: 10.1124/jpet.112.197756
This article has not been copyedited and formatted. The final version may differ from this version.

potently inhibited $EGFR^{WT}$ and $EGFR^{L858R}$ only. Compared with afatinib and canertinib, the reversible inhibitor lapatinib was 30-fold less potent on ErbB-4 and failed to inhibit $EGFR^{L858R/T790M}$ even at high concentrations.

We further characterized the binding properties of afatinib and BI 37781 using SPR technology at physiological pH (7.0). Tight binding to the EGFR targets prohibited accurate determination of rate constants but allowed for qualitative interaction analyses. Various interaction models were tested and compared to the 1:1 model ($E + I \leftrightharpoons EI$); of these, the induced-fit model was found to most accurately describe the complex interaction patterns observed (Figure 2). In this model the inhibitor forms an initial weak complex with the protein (EI), which then transforms into a tighter complex (EI*) ($E + I \leftrightharpoons EI \leftrightharpoons EI*$). The two EGFR variants differed mainly in the dissociation phases, with SPR sensorgrams showing a much slower dissociation from $EGFR^{WT}$ compared to $EGFR^{L858R/T790M}$ for both compounds. Afatinib dissociated more slowly from $EGFR^{L858R/T790M}$ compared with BI 37781 (Figure 2A). The SPR data also shows that under the present experimental conditions afatinib did not completely saturate all binding sites on the biosurface. Further binding analyses were performed at pH 8.0, reasoning that the cysteine 797 in EGFR would act as a stronger nucleophile thus favoring covalent bond formation. In line with this hypothesis, slower dissociation was observed at pH 8.0 compared with pH 7.0 for afatinib on both protein variants whereas BI 37781 displayed

essentially identical interaction patterns at both pH values (Figure 2B).

The crystal structure of the afatinib/EGFR kinase domain complex was solved at 2.8 Å resolution (R_{cryst}=20.5%, R_{free}=25.9%), revealing detailed binding interactions (Figure 3). The protein showed bilobal architecture characteristic for the protein kinase superfamily (Figure 3A) and structural results are in line with previously reported EGFR kinase domain data (Stamos et al., 2002). A rather long hydrogen-bond (3.3 Å) was formed between the amide nitrogen of Met^{793} at the hinge region and the quinazoline core of the inhibitor (Figure 3B). Most important, in addition to the non-covalent interactions, the electron density clearly showed a covalent bond formed between Cys^{797} at the edge of the active site and the Michael-acceptor group of afatinib. During the refinement process, the bond length for the C-S link was restrained to 1.82 Å. As shown in supplement Figure 3S1 the electron density unambiguously indicates the formation of the covalent C-S bond. The structure of the $EGFR^{T790M}$ mutant in complex with afatinib was also solved (PDB accession code 4G5P); however, the electron density around the dimethylamine group of afatinib was of lower resolution but suggested the formation of a covalent bond to Cys^{797}. For confirmation the use of alternative approaches to prove the covalent interaction with this EGFR mutant were performed.

JPET Fast Forward. Published on August 10, 2012 as DOI: 10.1124/jpet.112.197756
This article has not been copyedited and formatted. The final version may differ from this version.

For this purpose target-inhibitor complexes were analyzed by mass spectrometry (MS). The purified kinase domains of $EGFR^{WT}$, $EGFR^{L858R/T790M}$, HER2 and ErbB-4 were incubated with afatinib, digested with pepsin, and afatinib-peptide adducts were separated by liquid chromatography/mass spectrometry (LC/MS). The MS/MS spectra for all four constructs showed a peak at 520.17 Da that could be assigned to afatinib (486.18 Da) containing a protonated sulfur atom (34 Da) which originated from the respective Cys^{797} of EGFR, Cys^{805} of HER2 or Cys^{803} of ErbB-4 residues. For further confirmation, we compared the spectra resulting from a synthetic reference peptide derived from $EGFR^{L858R/T790M}$ and the peptic peptide adduct obtained under experimental conditions. The data reported in Figure 4 show that both spectra were essentially identical confirming that afatinib covalently engages the $EGFR^{L858R/T790M}$ mutant at residue 797. Similar MS/MS spectra were generated using the reference peptides for HER2 and ErbB-4, corroborating covalent modification at Cys^{805} and Cys^{803}, respectively (see Supplementary Material Figures 4S1 and 4S2 respectively). The identification of ion peaks corresponding to afatinib plus a sulfur atom and corresponding peptide adducts in the MS/MS spectra of EGFR (wild-type (not shown) as well as T790M), HER2 and ErbB-4 (Figure 4, 4S1 and 4S2) unequivocally demonstrates the ability of afatinib to form a covalent bond with all enzymatically active ErbB receptors. The observation that a peak representing an afatinib-cysteine adduct is lacking in both, the experimental sample and the

control peptide is best explained by the high fragmentation energy used in these experiments, a phenomenon which has been previously observed (Oberth et al.,1997; Sleno L et al., 2007).

Cellular Activity of ErbB Inhibitors. The differences between afatinib and its close analogue BI 37781 revealed by binding and enzymatic assays were more pronounced in cellular assays. Both compounds potently inhibited EGFR signaling (autophosphorylation assay in cancer cell lines expressing wild-type EGFR (A431: EC_{50} = 8 nM and 17 nM, respectively). Whereas afatinib also inhibited signaling in cell lines expressing mutant $EGFR^{L858R/T790M}$ (NCI-H1975: 49 nM) or HER2 (BT474: 75 nM), BI 37781 did not potently inhibit signaling in these cell lines displaying EC_{50} values above 500 nM. The difference in inhibitory profile was confirmed in proliferation assays where afatinib displayed nanomolar activity (NCI-H1975: 92 nM; BT474: 54 nM) whereas BI 37781 was ineffective even at high concentrations (>4000 nM). In agreeement with this observation, the irreversible inhibitor canertinib showed an inhibitory profile similar to afatinib, whereas the reversible inhibitors gefitinib, erlotinib showed activity similar to that of BI 37781 (Table 1). As afatinib has been shown to interact with and inhibit ErbB-4 protein expression as well as ErbB-4 phosphorylation was determined after 2 hours of incubation with kinase inhibitors in NIH3T3 mouse fibroblasts transfected with a plasmid encoding full-length ErbB-4 (Figure 5A). Inhibition of constitutive ErbB-4 phosphorylation by

afatinib started at 30 nM and was complete at 300 nM. While the covalent inhibitor canertinib showed full inhibition at 1000 nM, the non-covalent inhibitors lapatinib, gefitinib and erlotinib had no detectable effect on ErbB-4 phosphorylation at this concentration. Cellular washout experiments were performed to explore whether irreversible enzyme inhibition by covalently binding inhibitors results in prolonged duration of action. To this end, A431 cells expressing wild-type EGFR were incubated overnight in serum-free media to induce receptor dephosphorylation. Pretreatment with reversible and irreversible ErbB inhibitors at 300 nM for 1 hour prevented EGF-induced EGFR activation in all cases (Figure 5B). When the cells were washed after exposure to the inhibitors and incubated for 8 hours prior to addition of EGF, receptor phosphorylation was observed only in cells pretreated with reversible inhibitors (BI 37781, gefitinib), whereas activation was prevented in cells treated with irreversible inhibitors (afatinib, canertinib). A lag time of 24 to 48 hours was necessary for these cells to regain full sensitivity to EGF stimulation, in-line with the kinetics of *de novo* EGFR biosynthesis in this cell line (Decker 1984). These results suggest that covalent EGFR inhibitors might have advantages compared to reversible inhibitors due to their long lasting inhibition of receptor phosphorylation.

Discussion

Inhibition of aberrant ErbB receptor signaling has been at the forefront of personalized medicine in various indications including breast, colon, lung and stomach cancer. Targeted drugs including monoclonal antibodies (cetuximab, panitumumab, trastuzumab) and ATP-competitive kinase inhibitors (gefitinib, erlotinib, lapatinib) have been approved by health authorities. Newer chemical entities targeting ErbB receptors were designed to covalently engage their targets characterized by cysteine residues in the active site, assuming that this might translate into higher selectivity and longer residence time and, ultimately, into better efficacy (Copeland et al., 2007; Singh et al., 2011). The initial synthetic work by Fry and colleagues (Fry et al., 1994) on EGFR inhibitors paved the road for the development of such compounds. We have conducted a chemical synthesis program aiming for the discovery of irreversible inhibitors targeting all enzymatically active ErbB receptors in homo- as well as heterodimeric complexes, reasoning that drugs displaying a profile such as afatinib would provide an effective, long-lasting blockade of aberrant ErbB receptor signaling in multiple types of cancer. To more closely examine the role of irreversible target binding, we have synthesized a tool compound, BI 37781, which is almost identical in structure to afatinib except that the reactive double bond required for covalent binding to cysteine residues was replaced by a single bond.

Using SPR analysis as a biophysical approach to characterize drug-target interactions we observed that at pH 7.0, the sensorgrams of wild-type EGFR exposed to afatinib or BI 37781 were very similar. In contrast, afatinib dissociated more slowly than its analog from mutant $EGFR^{L858RT790M}$. Additional interaction analyses showed that at conditions favoring covalent bond formation (pH 8) afatinib dissociated more slowly from both wild-type and mutant targets than BI 37781, a result in line with covalent bond formation. X-ray crystallography of afatinib in complex with the kinase domain of wild-type EGFR unequivocally proved the formation of a covalent bond to Cys^{797} and also revealed that afatinib binds to the kinase in its active conformation. This binding mode contrasts with the one of lapatinib which reportedly requires the inactive conformation to accommodate the larger aromatic group attached to the aniline (Wood et al., 2004). The crystal structure of the $EGFR^{T790M}$ variant in complex with afatinib hinted towards covalent binding (PDB accession code 4G5P) and the binding mode was further investigated using mass spectrometry. Using this approach we could demonstrate the ability of afatinib to chemically react and form a covalent bond under physiological conditions (pH 7.5, 37°C) with EGFR, $EGFR^{L858R/T790M}$, HER2 and ErbB-4. However, because it had been reported that some types of covalent binding, such as Michael addition can be reversible (Lin et al., 2008) we wanted to show that covalent is also relevant in cancer cells. To this end, we invetsigated functional differences between afatinib and its analog BI 37781 in biological

systems and included additional, well-described tyrosine kinase inhibitors for comparison, including compounds capable of covalent binding (canertinib) as well as others (erlotinib, gefitinib, lapatinib) which – like BI 37781 – lack chemical reactivity. We observed that inhibition of proliferation of $EGFR^{L858R/T790M}$-containing lung cancer cells seems to require the presence of the Michael acceptor group (EC_{50} afatinib, canertinib: 0.1 µM; all other compounds: > 4 µM). As clonal emergence of $EGFR^{T790M}$ mutations is the cause of drug resistance in about 50% of non-small cell lung cancer patients relapsing on erlotinib or gefitinib treatment, these differences in potency may be of clinical relevance. In comparison to afatinib or canertinib, BI 37781 as well as erlotinib and gefitinib, were much less potent inhibitors of BT474 breast cancer cell proliferation that is known to be driven by over-expressed HER2. Lapatinib, in contrast, was almost as potent as the covalent binders, indicating that covalent target interaction is not essential for effective HER2 kinase inhibition. Afatinib was also identified as a potent inhibitor of ErbB-4 activity in cellular assays. Constitutive ErbB-4 phosphorylation in transfected NIH3T3 cells was blocked by afatinib and canertinib, but not by reversible inhibitors. Finally, we observed that the presence of the Michael acceptor group also resulted in prolonged duration of EGFR inhibition in cellular washout experiments. Signaling, as determined by measuring EGF-induced EGFR phosphorylation, was restored at least partially within 8 hours and to full extent within 24 hours of removal of reversible EGFR

binders. In contrast, restoration of kinase activity required up to 48 hours after wash-out of irreversible inhibitors, consistent with the hypothesis that kinase activity can only be restored by *de novo* biosynthesis of the receptor proteins. These results provide circumstantial evidence for a covalent bond formation in these cells and point to possible pharmacodynamic advantages of irreversibly binding inhibitors which could provide persistent target inhibition *in vivo* even after clearance of the drug from the system.

The plasticity of the ErbB network has recently been implicated in resistance to ErbB targeting agents such as cetuximab (Vlacich and Coffey, 2011) or trastuzumab (Narayan et al., 2009). *De novo* or acquired resistance to cetuximab can develop through receptor mutations (S492R; Montagut et al., 2012), ErbB2 amplification and increased heregulin synthesis (Yonesaka et al., 2011) or generation of HER2 isoforms by alternative splicing (e.g. 611-CTF [Quesnelle and Grandis, 2011]). Similarly, resistance to trastuzumab in breast carcinoma cells may be mediated by increased expression of EGFR and ErbB-3 (Narayan et al., 2009) as well as cognate ErbB ligands (Ritter et al., 2007) or truncated HER2 isoforms such as p95HER2 (Scaltriti et al., 2007). Our results indicate that afatinib is able to effectively silence aberrant ErbB network activity emanating from all homo- and heterotypic dimers formed; when used as a single agent or in drug combinations, afatinib thus may delay or prevent emergence of resistance due to ErbB reprogramming. Ongoing late-stage clinical trials evaluating the

efficacy and safety of afatinib in patients with cancers of the head and neck, lung (mutant EGFR) and breast (amplified HER2) will ultimately reveal whether the distinct pharmacological features of this compound translate into improved patient benefit.

Acknowledgements

Beactica AB, Uppsala, Sweden is gratefully acknowledged for performing the SPR experiments. We would also like to thank all present and past members of the Afatinib research and development teams and their collaborators for excellent technical contributions and Dr. Jürgen Moll for diligent and critical reviewing.

Authorship contributions

Participated in research design: Bader, Dahl, Haaksma, Klein, Kraemer, Sanderson, Solca, Zoephel
Conducted experiments: Solca, Zoephel
Contributed to new reagents or analytic tools: Himmelsbach
Performed data analysis: Solca, Dahl, Zoephel, Bader, Adolf, Sanderson,
Wrote or contributed to the writing of the manuscript: Solca, Dahl, Zoephel, Bader, Adolf

References

Alvarado D, Klein DE, and Lemmon MA (2009) ErbB2 resembles an autoinhibited invertebrate epidermal growth factor receptor. *Nature* **461**: 287–291.

Bang YJ, Van Cutsem E, Feyereislova A, Chung HC, Shen L, Sawaki A, Lordick F, Ohtsu A, Omuro Y, Satoh T, Aprile G, Kulikov E, Hill J, Lehle M, Rüschoff J, and Kang YK (2009) Trastuzumab in combination with chemotherapy versus chemotherapy alone for treatment of HER2-positive advanced gastric or gastro-oesophageal junction cancer (ToGA): a phase 3, open-label, randomised controlled trial. *Lancet* **376**: 687–697.

Collaborative Computational Project, Number 4 (1994) The CCP4 Suite: Programs for Protein Crystallography. *Acta Cryst* **D50**: 760–763.

Copeland RA, Pompliano DL, and Meek TD (2007) Drug–target residence time and its implications for lead optimization. *Nat Rev Drug Discov* **5**: 730–739.

Decker SJ (1984) Aspects of the metabolism of the epidermal growth factor receptor in A431 human epidermoid carcinoma cells. *Mol Cell Biol* **4**: 571–575.

Dengler WA, Schulte J, Berger DP, Mertelsmann R, and Fiebig HH (1995) Development of a propidium iodide fluorescence assay for proliferation and cytotoxicity assays. *Anticancer Drugs* **6**: 522–532.

Eck MJ and Yun CH (2010) Structural and mechanistic underpinnings of the differential drug sensitivity of EGFR mutations in non-small cell lung cancer. *Biochim Biophys Acta* **1804**: 559–566.

Emsley P, Lohkamp B, Scott WG, and Cowtan K. (2010) Features and development of Coot. *Acta Cryst* **D66:** 486–501.

Fry DW, Kraker AJ, McMichael A, Ambroso LA, Nelson JM, Leopold WR, Connors RW, and Bridges AJ (1994) A specific inhibitor of the epidermal growth factor receptor tyrosine kinase. *Science* **265**: 1093–1095.

Garrett TPJ, McKern NM, Lou M, Elleman TC, Adams TE, Lovrecz GO, Kofler M, Jorissen RN, Nice EC, Burgess AW, and Ward CW (2003) The crystal structure of a truncated ErbB2 ectodomain reveals an active conformation, poised to interact with other ErbB receptors. *Mol Cell* **11**: 495–505.

Graus-Porta D, Beerli RR, Daly JM, and Hynes NE (1997) ErbB-2, the preferred heterodimerization partner of all ErbB receptors, is a mediator of lateral signaling. *EMBO J* **16**: 1647–1655.

Ji H, Zhao X, Yuza Y, Shimamura T, Li D, Protopopov A, Jung BL, McNamara K, Xia H, Glatt KA, Thomas RK, Sasaki H, Horner JW, Eck M, Mitchell A, Sun Y, Al-Hashem

R, Bronson RT, Rabindran SK, Discafani CM, Maher E, Shapiro GI, Meyerson M, and Wong KK (2006) Epidermal growth factor receptor variant III mutations in lung tumorigenesis and sensitivity to tyrosine kinase inhibitors. *Proc Natl Acad Sci USA* **103**: 7817–7822.

Kabsch W (2010) Integration, scaling, space-group assignment and post-refinement. *Acta Cryst* **D66**: 133–144.

Li D, Ambrogio L, Shimamura T, Kubo S, Takahashi M, Chirieac LR, Padera RF, Shapiro GI, Baum A, Himmelsbach F, Rettig WJ, Meyerson M, Solca F, Greulich H, and Wong KK(2008) BIBW2992, an irreversible EGFR/HER2 inhibitor highly effective in preclinical lung cancer models. *Oncogene* **27**: 4702–4711.

Lin D, Saleh S, and Liebler DC (2008) Reversibility of covalent electrophile-protein adducts and chemical toxicity. *Chem Res Toxicol* 21: 2361–2369.

Lynch TJ, Bell DW, Sordella R, Gurubhagavatula S, Okimoto RA, Brannigan BW, Harris PL, Haserlat SM, Supko JG, Haluska FG, Louis DN, Christiani DC, Settleman J, and Haber DA (2004) Activating mutations in the epidermal growth factor receptor underlying responsiveness of non-small-cell lung cancer to gefitinib. *N Engl J Med* **350**: 2129–2139.

Montagut C, Dalmases A, Bellosilo B, Crespo M, Pairet S, Iglesisas M, Salido M, Gallen M, Marsters S, Ping Tsai S, Minoche A, Somasekar S, Serrano S, Himmelbauer H, Bellmunt J,

Rovira A, Settlemann J, Bosch F, and Albanell J (2012) Identification of a mutation in the extracellular domain of the Epidermal Growth Factor Receptor conferring cetuximab resistance in colorectal cancer. *Nat Med* **18**: 221–223.

Narayan M, Wilken JA, Harris LN, Baron AT, Kimbler KD, and Maihle NJ (2009) Trastuzumab-Induced HER Reprogramming in "Resistant" Breast Carcinoma Cells. *Cancer Res* **69**: 2191–2194.

Oberth CA and Jones AD (1997) Fragmentation of protonated thioether conjugates of acrolein using low collision energies. *J Am Sot Mass Spectrom* **8**: 727–736.

Prickett TD, Agrawal NS, Wie X, Yates KE, Lin JC, Wunderlich JR, Cronin JC, Cruz P, Rosenberg SA, and Samuels Y (2009) Analysis of the tyrosine kinome in melanoma reveals recurrent mutations in ERBB4. *Nat Genetics* **41**: 1127–1132.

Quesnelle KM and Grandis JR (2011) Dual kinase inhibition of EGFR and HER2 overcomes resistance to cetuximab in a novel in vivo model of acquired cetuximab resistance. *Clin Cancer Res* **17**: 5935–44.

Ritter CA, Perez-Torres M, Rinehart C, Guix M, Dugger T, Engelman JA, and Arteaga CL (2007) Human Breast Cancer Cells Selected for Resistance to Trastuzumab In vivo Overexpress Epidermal Growth Factor Receptor and ErbB Ligands and Remain Dependent on

the ErbB Receptor Network. *Clin Cancer Res* **13**: 4909–4919.

Scaltriti M, Rojo F, Ocana A, Anido J, Guzman M, Cortes J, Di Cosimo S, Matias-Guiu X, Ramon y Cajal S, Arribas J, and Baselga J (2007) Expression of p95HER2, a truncated form of the HER2 receptor, and response to anti-HER2 therapies in breast cancer. *J Natl Cancer Inst* **99**: 628–638.

Singh J, Petter RC, Baillie TA, and Whitty A (2011) The resurgence of covalent drugs. *Nat Rev Drug Discov* **10**: 307–317.

Slamon DJ, Clark GM, Wong SG, Levin WJ, Ullrich A, and McGuire WL (1987) Human breast cancer: correlation of relapse and survival with amplification of the HER-2/neu oncogene. *Science* **235**: 177–182.

Sleno L, Varesio E, and Hopfgartner G (2007) Rapid commun. *Mass Spectrom* **21**: 4149–4157.

Solca FF, Baum A, Langkopf E, Dahmann G. Heidr KH, Himmelsbach F, and van Meel JCA (2004) Inhibition of epidermal growth factor receptor activity by two pyrimidopyrimidine derivatives. J Pharmacol Exp Ther **311**: 502–509.

Stamos J, Sliwkowski MX, and Eigenbrot C (2002) Structure of the epidermal growth factor receptor kinase domain alone and in complex with a 4-anilinoquinazoline inhibitor. *J Biol Chem* **277**: 46265–46272.

Tzahar E, Waterman H, Chen X, Levkowitz G, Karunagaran D, Lavi S, Ratzkin BJ, and Yarden Y (1996) A hierarchical network of interreceptor interactions determines signal transduction by Neu differentiation factor/neuregulin and epidermal growth factor. *Mol Cell Biol* **16**: 5276–5287.

Vlacich G and Coffey RJ (2011) Resistance to EGFR-Targeted Therapy: A Family Affair. *Cancer Cell* **20**: 423–425.

Wood ER, Truesdale AT, McDonald OB, Yuan D, Hassell A, Dickerson SH, Ellis B, Pennisi C, Horne E, Lackey K, Alligood KJ, Rusnak DW, Gilmer TM, and Shewchuk L (2004) A unique structure for epidermal growth factor receptor bound to GW572016 (Lapatinib): relationships among protein conformation, inhibitor off-rate, and receptor activity in tumor cells. *Cancer Res* **64**: 6652–6659.

www.clinicaltrials.gov

Yarden Y and Sliwkowski MX (2001) Untangling the ErbB signalling network. *Nat Rev Mol Cell Biol* **2**: 127–137.

Yonesaka K, Zejnullahu K, Okamoto I, Satoh T, Cappuzzo F, Souglakos J, Ercan D, Rogers A, Roncalli M, Takeda M, Fujisaka Y, Philips J, Shimizu T, Maenishi O, Cho Y, Sun J, Destro A, Taira K, Takeda K, Okabe T, Swanson J, Itoh H, Takada M, Lifshits E, Okuno

K, Engelman JA, Shivdasani RA, Nishio K, Fukuoka M, Varella-Garcia M, Nakagawa K, and Jänne PA (2011) Activation of ERBB2 Signaling Causes Resistance to the EGFR-Directed Therapeutic Antibody Cetuximab. *Sci Transl Med* **3**: 99ra86

Yun C.H, Mengwasser KE, Toms AV, Woo MS, Greulich H, Wong KK, Meyerson M, and Eck MJ (2008) The T790M mutation in EGFR kinase causes drug resistance by increasing the affinity for ATP. *Proc Natl Acad Sci U S A* **105**: 2070–2075.

Zhang H, Berezov A, Wang Q, Zhang G, Drebin J, Murali R, and Greene MI (2007) ErbB receptors: from oncogenes to targeted cancer therapies. *J Clin Invest* **117**: 2051–2058.

Zhang X, Gureasko J, Shen K, Cole PA, and Kuriyan J (2006) An allosteric mechanism for activation of the kinase domain of epidermal growth factor receptor *Cell* **125**: 1137–1149.

Footnotes

Current affiliation: AstraZeneca R&D, Mölndal, Sweden (G.D.)

Financial support: The work was entirely supported by Boehringer-Ingelheim.

For reprint requests, contact:

Flavio Solca

Address: Doktor-Böhringer-Gasse 5-11, A-1120, Vienna, Austria

E-mail: flavio.solca@boehringer-ingelheim.com

Conflict of interest: All authors are or were employees of Boehringer Ingelheim. No potential conflicts of interest.

Figure Legends

Figure 1: Structures of chemical entities targeting ErbB receptor family members. Panel (**A**) describes the postulated covalent mode of binding of afatinib to a reactive cysteine and panel (**B**) shows the structures of the small molecule kinase inhibitors used in this study.

Figure 2: Surface plasmon resonance sensorgrams show that afatinib binding follows an induced fit mechanism. The y-axis shows the normalized responses and the x-axis shows the elapsed time. The compounds were analyzed at a concentration of 200 nMwith a contact time of 300 seconds followed by 600 seconds dissociation. **A.** Fitting of the 1:1 model ($E + I \leftrightharpoons EI$, left panel) or the induced fit model ($E + I \leftrightharpoons EI \leftrightharpoons EI*$, right panel) to sensorgrams obtained using BI 37781 and afatinib on wild type (red) or L858R/T790M (cyan) variants of the EGFR kinase domain. The fitted interaction models are shown in black. **B.** Interaction of BI 37781 and afatinib with wild type or L858R/T790M variants of EGFR kinase domain at pH 7.0 (red) or pH 8.0 (blue).

Figure 3: Crystal structure of wild type EGFR (residues G696-G1022) in complex with afatinib. The insert (A) shows the structure of the whole EGFR kinase domain. A close up of

the hinge region is shown in (B).The dotted line represents a 3.3 Å hydrogen-bond formed between the amide nitrogen of Met^{793} at the hinge region and the quinazoline core of afatinib. Tables showing the statistics of data collection and processing as well as refinement statistics can be found in the *supplementary material* section Figure 3S2.

Figure 4: Comparison of fragmentation mass spectra (MS/MS) demonstrates covalent binding of afatinib to $EGFR^{T790M/L858R}$. (**A**) Chemically synthesized EGFR peptide amino acids 791-798, covalently modified with afatinib and (**B**) the corresponding peptide, isolated from the $EGFR^{T790M/L858R}$ kinase domain after incubation with afatinib were resolved by liquid chromatography/tandem mass spectrometry. The peptide sequence was derived from information of b- and y-ion fragmentation series, isotopic distribution patterns of fragments as well as the mass of the parent ion. Identified ions of the b- and y-ion fragmentation series have been annotated.

Figure 5: Cellular experiments confirm ErbB-4 inhibition and prolonged duration of action of afatinib on EGFR. (A) NIH3T3 cells transiently transfected with an ErbB-4 expression vector (48 h) were incubated with kinase inhibitors for 2 h before lysis. The resulting extracts (50 µg per lane) were resolved by SDS-PAGE, transferred to PVDF membranes and

probed with the rabbit monoclonal antibodies 83B10 (HER4) and 21A9 (phosphorylated ErbB-4; Tyr1284). (**B**) A431 cells were incubated with inhibitors at a final concentration of 300 nM in serum free media for 1 h before stimulation with 100ng/ml EGF. The bars in the graph (mean of 6 replicates) represent the EGFR phosphorylation status at different time points after drug washout.

Table

Table 1. Potency of ErbB receptor inhibitors in molecular and cellular assays - The inhibitory constants were determined as described in "Materials and Methods". All values were derived from technical duplicates and confirmed in multiple (n) independent biological experiments. Values in bold were determined in the same experiment to allow direct comparison. The range of confirmatory values wich comprise 197 independent EC_{50} determinations includes 16 EC_{50} values previously reported (Li et al. (2008)) marked with an asterix.

		Compounds					
	IC_{50} [nM]	**Afatinib**	**BI 37781**	**Lapatinib**	**Canertinib**	**Erlotinib**	**Gefinitib**
ErbB-4 kinase	Value	**1**	**544**	**30**	**1**	**579**	**323**
	Range	0.7-1.7	510-544	18-30	0.8-10	579-756	293-323
	(n)	4	2	3	4	2	2

$EGFR^{WT}$ kinase	Value	**0.5**	**0.8**	**-**	**-**	**-**	**-**
	Range	0.2-0.7	0.8-1	0.3-17	0.3*-1.7	0.9-1.7	0.4-4.7
	(n)	5	2	6	5	4	6
$EGFR^{L858R}$ kinase	Value	**0.2**	**1**	**-**	**-**	**-**	**-**
	Range	0.2-0.4*	1-2	2-8*	0.4-0.8*	1.1-2.7	0.8-000
	(n)	2	2	3	2	3	2
$EGFR^{L858R/T790M}$ kinase	Value	**9**	**57**	**-**	**-**	**-**	**-**
	Range	9-10*	36-57	>4000	18-36	1520-3562	534-1267
	(n)	2	2	3	3	3	4
HER2 kinase	Value	**14**	**84**	**-**	**-**	**-**	**-**
	Range	7-25	84-112	6-25	22-72	238-698	416-1830
	(n)	5	2	4	3	3	6

Phospho EGFR (A431)	Value	**8**	**17**	**-**	**-**	**-**	**-**
EGFR WT kinase	Range	8-13*	17-56	93-145	17-22*	3-8	22-63
	(n)	4	2	4	5	5	4
Phospho EGFR	Value	**49**	**1610**	**-**	**-**	**-**	**-**
(NCI-H1975)	Range	49-129	1458-1610	>4000*	76-88	>4000*	>4000*
EGFR L858R/T790M	(n)	5	2	2	3	3	3
Phospho HER2 (BT474)	Value	**75**	**570**	**-**	**-**	**-**	**-**
HER2 gene ampl.	Range	35*-75	570-1237	74-102	88-184*	396-930	3600-3710*
	(n)	5	3	3	2	3	2
Proliferation (NCI-H1975)	Value	**92**	**>3000**	**-**	**-**	**-**	**-**
L858R/T790M (3D assays)	Range	92-225	>3000	>4000*	57-307	>4000*	>4000*
	(n)	4	2	2	4	3	3

Proliferation (BT474)	Value	**54**	**>4000**	**-**	**-**	**-**	**-**
HER2 gene ampl.	Range	12-56	>4000	12-128	37-66	599-899	1070-1960
(2D assays)	(n)	5	3	3	3	3	3

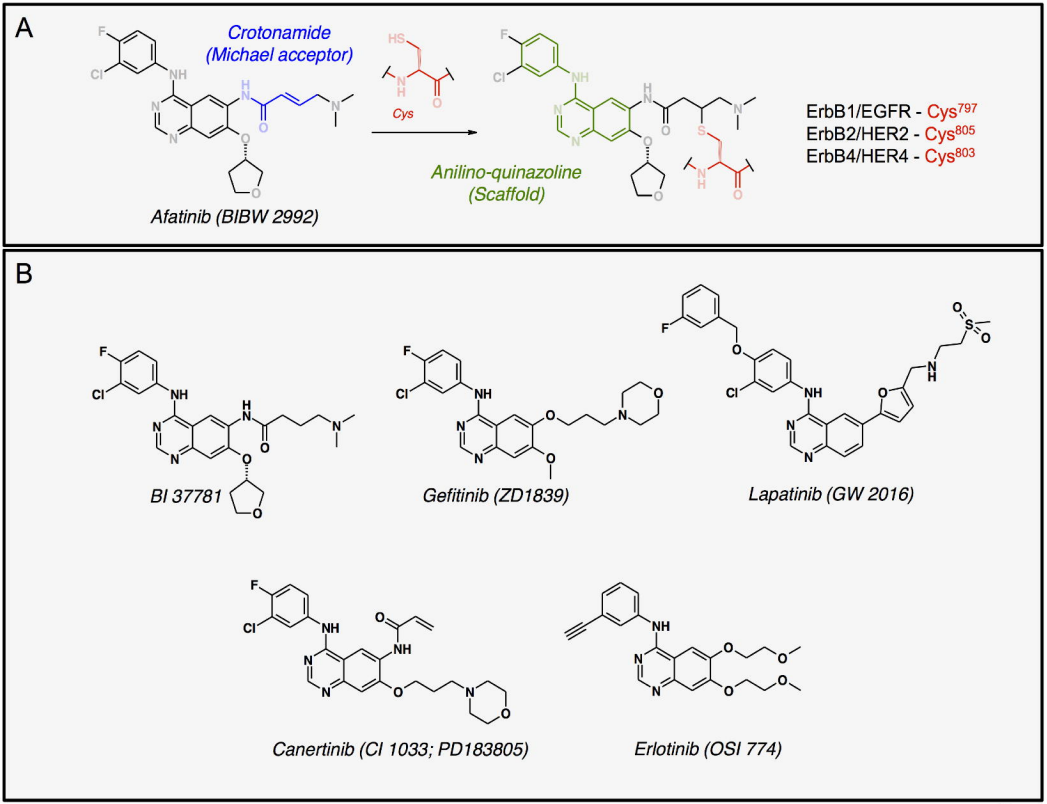
A
Crotonamide
(Michael acceptor)
Cys
Anilino-quinazoline
(Scaffold)
Afatinib (BIBW 2992)
ErbB1/EGFR - Cys797
ErbB2/HER2 - Cys805
ErbB4/HER4 - Cys803
B
BI 37781
Gefitinib (ZD1839)
Lapatinib (GW 2016)
Canertinib (CI 1033; PD183805)
Erlotinib (OSI 774)

Figure 1

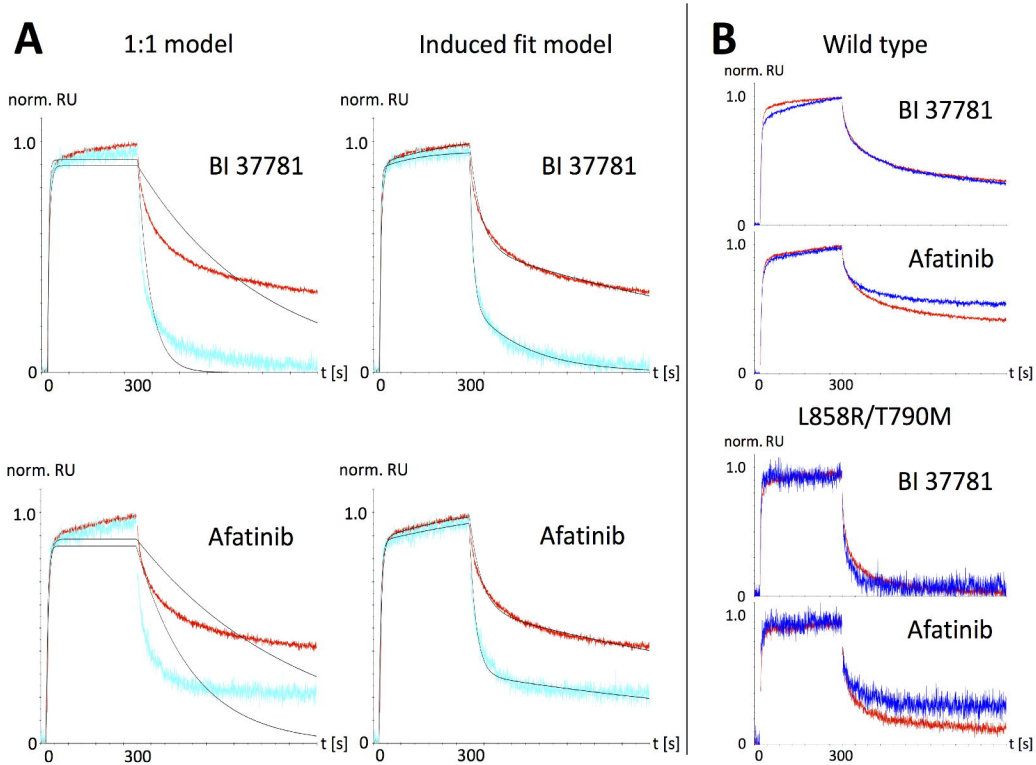
A
1:1 model
Induced fit model
norm. RU
1.0
0
BI 37781
Afatinib
0
300
t [s]
B
Wild type
L858R/T790M

Figure 2

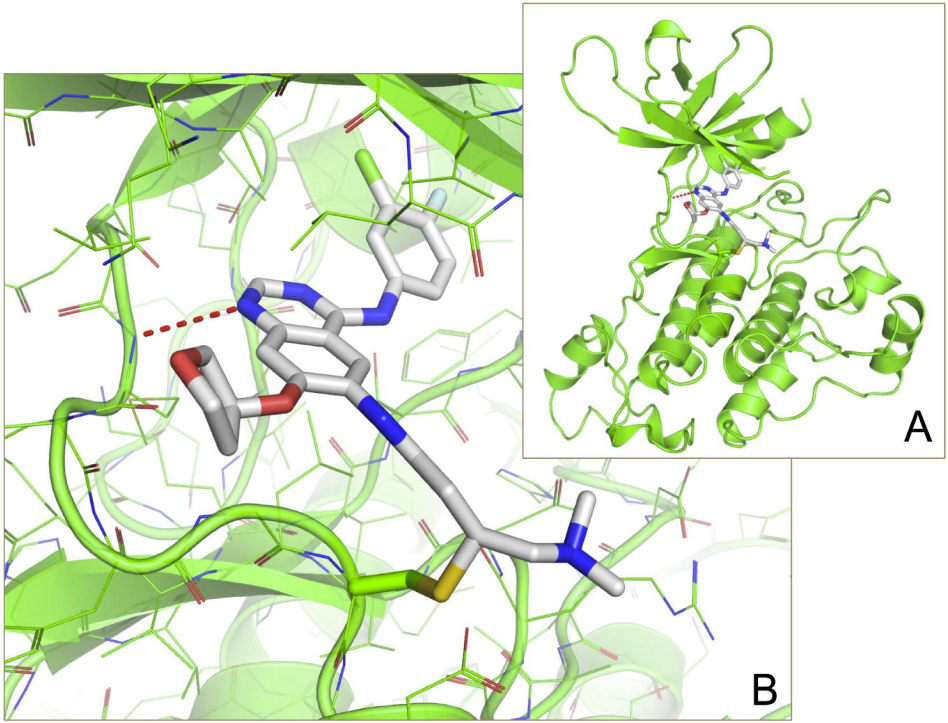

Figure 3

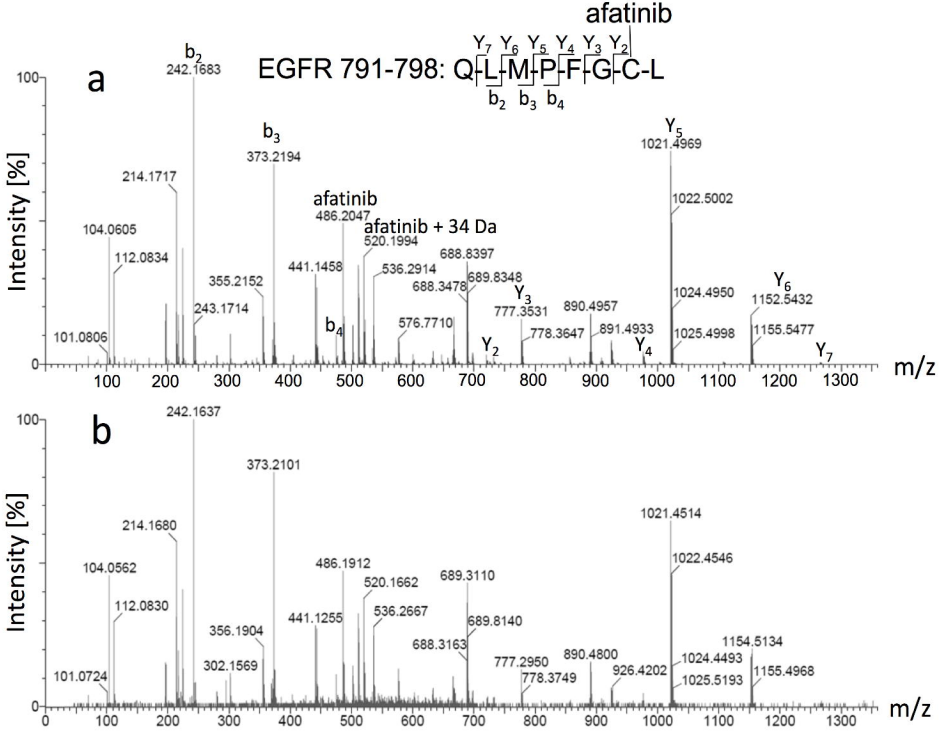
afatinib
EGFR 791-798: Q-L-M-P-F-G-C-L
a
b
Intensity [%]
m/z
242.1683
373.2194
214.1717
104.0605
112.0834
101.0806
355.2152
243.1714
441.1458
486.2047
afatinib
520.1994
afatinib + 34 Da
536.2914
688.8397
689.8348
688.3478
576.7710
777.3531
778.3647
890.4957
891.4933
1021.4969
1022.5002
1024.4950
1025.4998
1152.5432
1155.5477
242.1637
373.2101
214.1680
104.0562
112.0830
101.0724
356.1904
302.1569
486.1912
520.1662
536.2667
441.1255
689.3110
689.8140
688.3163
777.2950
778.3749
890.4800
926.4202
1021.4514
1022.4546
1024.4493
1025.5193
1154.5134
1155.4968

Figure 4

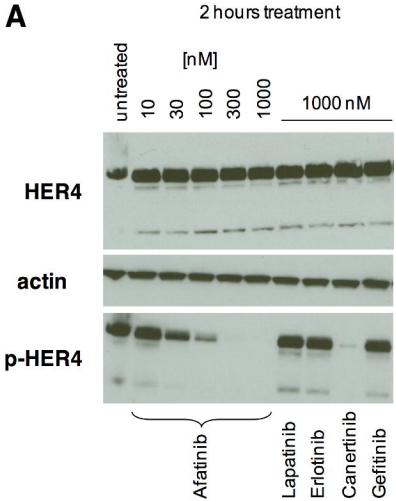
A
2 hours treatment
untreated
[nM]
10
30
100
300
1000
1000 nM
HER4
actin
p-HER4
Afatinib
Lapatinib
Erlotinib
Canertinib
Gefitinib

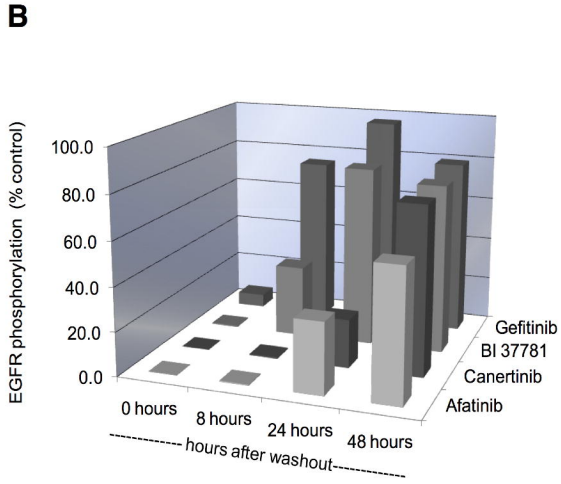
B
EGFR phosphorylation (% control)
100.0
80.0
60.0
40.0
20.0
0.0
0 hours
8 hours
24 hours
48 hours
hours after washout
Gefitinib
BI 37781
Canertinib
Afatinib

Figure 5